A PACKAGED SILICON MEMS VIBRATORY GYROSCOPE FOR MICROSPACECRAFT

Tony K. Tang, Roman C. Gutierrez, Christopher B. Stell, Vatche Vorperian, Genji A. Arakaki, John T. Rice, Wen J. Li, Indrani Chakraborty, Kirill Shcheglov, Jaroslava Z. Wilcox
Jet Propulsion Laboratory
MicroDevices Laboratory, California Institute of Technology
4800 Oak Grove, Pasadena, CA 91109-8099

William J. Kaiser
Department of Electrical Engineering
University of California, Los Angeles, CA 90024-1594

ABSTRACT

In this paper, we present recent work on the design, fabrication, and packaging of a silicon Micro-Electro-Mechanical System (MEMS) microgyroscope designed for space applications. A hermetically sealed package that houses the microgyroscope and most of its control electronics has been built and tested. The entire micro-gyroscope package is approximately 1 x 1 x 0.7 inches in dimensions. The rest of the control electronics which includes the drive and lock-in amplifier circuitry are mounted outside the gyro box on a 1 x 1 inch circuit board. This packaged microgyroscope has a 7 Hz split between its drive and sense mode and has a scale factor of 24mV/deg/sec, bias stability of 70 deg/hr, angle random walk of 6.3 deg/$\sqrt{\text{hr}}$, and a rate ramp of 0.2 deg/hr/sec. Recent improvements on the fabrication and assembly procedures and microgyroscope design have resulted in clover-leaf structures with matched drive and sense resonant frequency. These new structures have a very small temperature dependent frequency shift of 0.23 Hz/degree for both the drive and sense modes.

INTRODUCTION

Future space exploration missions will require micro-spacecraft that are 10 to 1000 times lower in cost, mass, volume, and power consumption than present generation of spacecraft such as the Galileo and the Cassini spacecraft. These drastic reductions lead to similiar changes in the attitude control system of the spacecraft. Attitude control systems that use conventional gyroscope technologies are exceedingly costly, massive, and consume too much power to be used in the new microspacecraft designs. Micromachined vibratory gyro-scopes [1,2,3,4] are promising candidates to replace conventional gyroscopes for use in this new generation of microspacecraft because these new microgyroscopes are small (<30gm entire package), sensitive (1-100 deg/hr), consume little power (<0.5W), and much less expensive than alternate technologies.

DESCRIPTION

Previously, we demonstrated a new silicon micromachined gyroscope with a bias stability of 29 deg/hr and a minimum resolution of 90deg/hr at 1 second integration time using external "rack" electronics [1]. This silicon microgyroscope resembles a four leaf clover suspended by four thin wires with a metal post attached to the center (Figure 1). The clover leaves provide large areas for electrostatic drive and sensing at the lowest resonant modes. The post provides a large Coriolis force coupling between the orthogonal normal modes when the gyroscope rotates about the post axis.

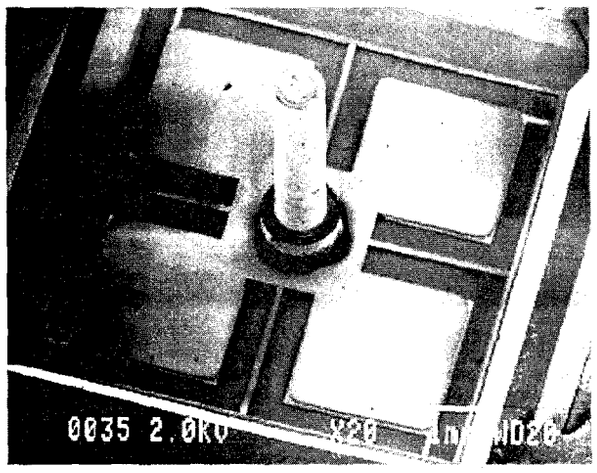

Figure 1. SEM picture of an assembled silicon micromachined gyroscope.

The highest rotation sensitivity for a vibratory gyroscope is obtained when the two oscillatory modes (drive and sense) have the same resonant frequency. The response to the Coriolis acceleration is then amplified by the Q factor of the resonance resulting in improved sensor performance and reduced drive voltage. The drive and sense modes are inherently degenerate for the clover-leaf structure is symmetrical in the x-y plane. This allows us to take advantage of the Q-amplification of the clover-leaf displacements.

FABRICATION

Bulk silicon micromachining technology is used to manufacture the clover-leaf vibratory microgyroscope. The microgyroscope consists of three major

components: the silicon clover-leaf structure, the silicon baseplate, and the metal post. The fabrication steps of the silicon clover-leaf structure and the baseplate are almost identical, involving two masking and etching steps and one metallization step. The starting material for both the clover-leaf structure and the baseplate are p-type <100> double-side polished silicon of moderate doping (1-3 ohm-cm) with two epilayers grown on top. The buried epilayer is 4 microns thick doped with Boron ($10^{20}/cm^3$) and counter-doped with Ge for stress relief. The top epilayer is 26 microns thick. This epilayer is heavily As-doped for the clover-leaf structure and n-doped for the baseplate.

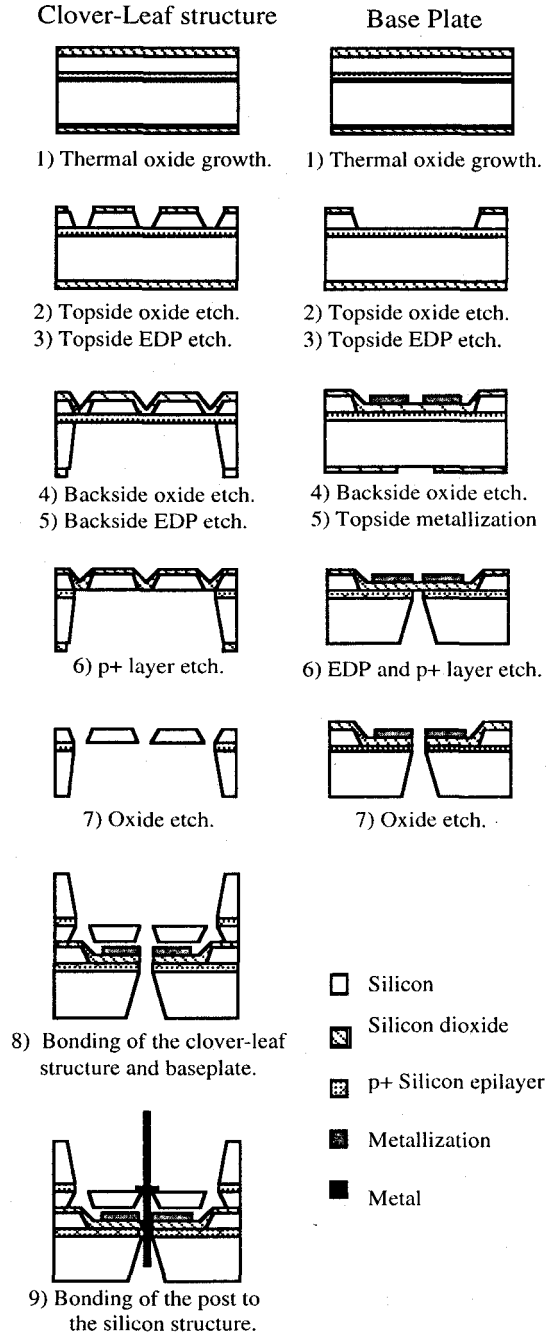

Figure 3. Fabrication process for the silicon clover-leaf structure and the silicon base plate.

The fabrication process sequence for the microgyroscope is shown in Figure 3. A thin layer (1000Å) of thermal oxide is grown on the wafer and patterned with the clover leaf pattern. This patterned oxide layer is used as a mask for EDP etching of the 26 microns silicon epilayer to the p+ etch-stop layer. The crystal plane selectivity of the anisotropic EDP etch provides very precise and smooth dimensions and surfaces for clover-leaf structure. After the EDP etch, the thin thermal oxide mask is stripped away and another 3000Å thick thermal oxide is grown on the wafer. The silicon dioxide layer on back of the wafer is then patterned and the device is again etched in EDP. This etch removes all the silicon substrate and stops at the p+ etch-stop layer. Next, the wafer is cleaved into individual devices and separated. The cleaved devices are then reactive ion etched with SF_6 and O_2 until the p+ stop-etch layer is removed. Finally, the oxide layer is striped away using CF_4 and O_2 plasma.

The fabrication process of the silicon base plate is similar to that used for the fabrication of the clover-leaf structure but with an additional metallization step for the electrodes. The gap spacing which separates the clover-leaf structure and the electrodes on the baseplate is realized by the first EDP etch in the baseplate processing sequence. After the clover-leaf structure and the baseplate are separately fabricated, they are then bonded together. All devices are first tested for resonant frequencies and mode shapes. After these initial tests, a metal post is epoxied into the hole on the silicon resonator (Figure 4). The dimension of the silicon clover-leaf structure is 7 mm x 7 mm, the dimension of each clover leaf is 1.8 mm x 1.8 mm, and the post is 500 microns in diameter and 5 mm in length. The silicon base plate is 1 cm x 1 cm and is approximately 400 microns thick.

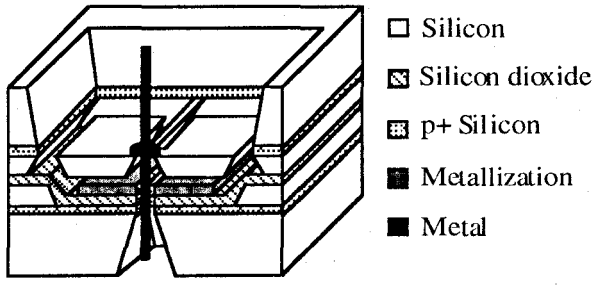

Figure 4. Cross-sectional view of the complete microgyroscope.

CONTROL AND ELECTRONICS

Block diagram and operation

The block diagram for the microgyroscope electronics is shown in figure 5 in which the four shaded squares represent the gyroscope's four capacitive ports. Two of the ports are used as electrostatic drive inputs and two are used for sensing the motion of the structure. The summing and difference amplifiers are represented by the

circular nodes. The sum amplifier provides a signal that is due to resonator motion along the driven axis, while the difference amplifier provides a signal that is due to resonator motion along the sense axis produced by rotation. The block labeled "H(s)" represents a voltage gain circuit. It is controlled by the automatic gain control circuit represented by the "AGC" block.

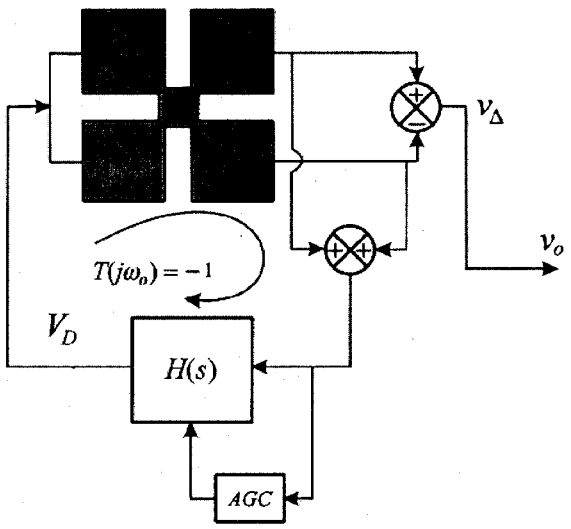

Figure 5. Block diagram of the microgyroscope control electronics.

The microgyroscope is driven into a rocking resonant mode by amplifying and feeding back the sum amplifier signal to the drive ports. The AGC circuit in conjunction with the voltage controlled amplifier circuit sets the drive voltage amplitude as necessary to maintain the desired peak to peak displacement. In the absence of rotation, the rocking motion of the structure is confined to the driven axis, the difference signal is therefore zero. Under rotation about the axis perpendicular to the plane formed by the sense and drive axes, the Coriolis effect causes the rocking motion in the drive axis to couple to the sense axis. The amplitude of the resulting difference signal is proportional to the applied rotation rate. The displacements in the sense axis due to the Coriolis force is small in comparison to the displacements in the drive axis, thus, the sense signal is small compared to the drive signal and easily obscured by electrical noise and parasitic coupling of drive signal. For this reason synchronous detection at 90° from the drive signal is used to extract the desired Coriolis induced signal.

Effect of Q-factor

Increasing the Q factor of the resonator has the desirable effect of increasing the sensitivity of the micro-gyroscope and the undesirable effect of increasing the required dynamic range of the AGC circuitry. As the resonator Q factor is increased the difference between the gain required to start resonance and maintain resonance increases. High gains during startup can lead to undesirable high frequency electrical oscillations which can prevent proper electromechanical resonance. One precaution that can be taken is to reduce the gain of the voltage controlled amplifier at frequencies above resonance.

Preamplifier

The preamplifier consists of a pair of low current noise amplifiers, one for each of the two sense ports. Metal film high megohm resistors were chosen for the resistors due to their superior noise performance over their thick film counterparts. Unshielded long interconnections between the microgyroscope's sense ports and the amplifiers can cause problems, especially if the interconnections are not rigidly supported. Vibration induced flexure can cause generation of unwanted signals due to changing parasitic capacitances. The amplifier is extremely sensitive to capacitance changes on its input. One gigaohm of resistance between the sense and drive electrodes can cause excessive coupling of the drive signal into the sense amplifiers. The microgyroscope baseplate and all electronic components associated with the preamplifier must be free of contamination. We have fabricated the preamplifier circuitry using surface mount components on conventional glass printed wire boards and using hybrid techniques in which bare die were attached to a fired ceramic substrate. Both techniques offered good performance, but the hybrid performed noticeably better.

ASSEMBLY AND PACKAGING

The goal of this packaging design is to build a small package to house the microgyroscope, a pre-amplifier circuit, a summing/subtracting circuit and a small voltage regulator/power converter. In addition, the micro-gyroscope needs to be operated in a vacuum of 10^{-2} to 10^{-3} torr, necessitating a hermetic package. The initial goal is to create a sufficient seal for the package such that, with an initial vacuum on the order of 10^{-6} torr, vacuum would be held for 2-3 months. Since this package is for spaceflight applications, the design must also address the environmental conditions of spaceflight.

To minimize the package's size, a double-sided substrate (parts on both sides) was developed. This ameliorated the impact of the larger capacitor form factors (.22 x .25 inch) necessary in the circuit. Without the use of multilayer substrates, two single sided substrates were designed and mounted back to back. These substrates were connected using ribbon conductors, complicating the edges of the substrates (where the connections between substrates were made). A gold-plated, brass package was designed, utilizing soldered, hermetic feed-throughs and a solder-seal lid. To improve the seal effectiveness, the package to lid interface was designed as a simple labyrinth seal (Figure 7). The solder feed-throughs selected were from available stock (again, in the interest of time), but were specified to be 10^{-8} cc/sec leak rate or better. The final enclosure size was 1.1 x 1.0 x 0.7 inches. The completed microgyroscope package is shown in figure 8. Figure 9 shows the

constituent parts of the assembly, including two substrates, a metal enclosure and lid, and hermetic solder feed-throughs.

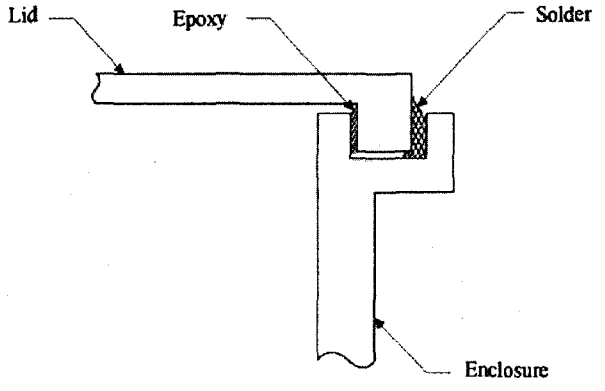

Figure 7. Labyrinth seal design for the package lid interface.

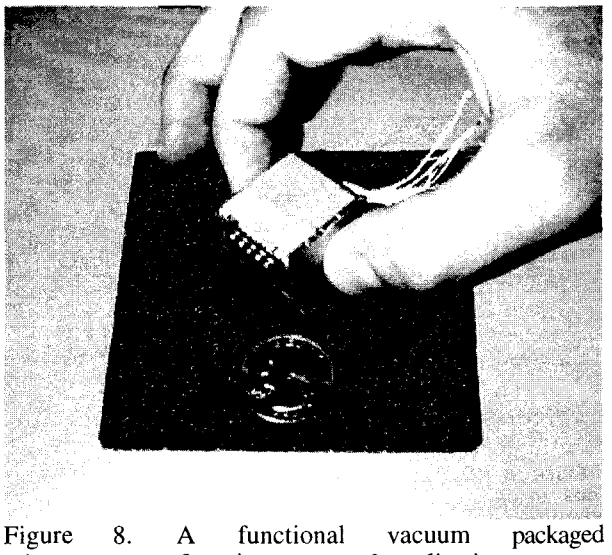

Figure 8. A functional vacuum packaged microgyroscope for microspacecraft applications.

The substrates were mounted to the package using a combination of fasteners (0.8 UNM) and adhesive. Originally envisioned as a reworkable package, the adhesive bonding was added later to reduce the torque required on the fasteners (used as locating devices only), thus minimizing the stress on the ceramic substrates. The package also incorporated provisions for a pinch-off tube, which was used to generate the final seal in a vacuum environment. Electrical components were bonded to the substrates and electrical connections made via gold wire-bonds.

While the power dissipation of individual devices within the package are not significant, the cumulative power dissipation was high enough to warrant further investigation. After the initial design was complete, a simple ANSYS finite-element thermal model was generated. The results of this analysis are shown in figure 10. These results indicate that significant temperatures rises will not occur within the package.

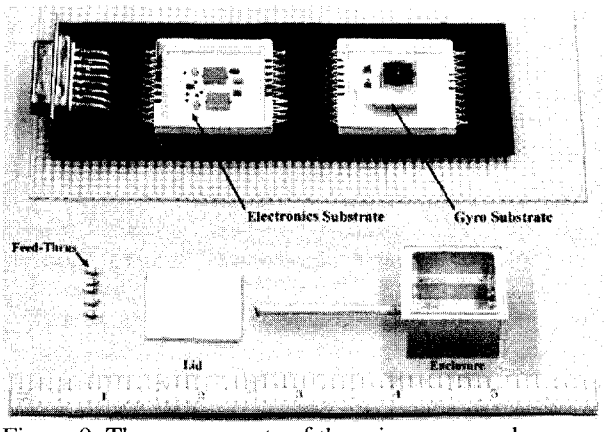

Figure 9. The components of the microgyro package.

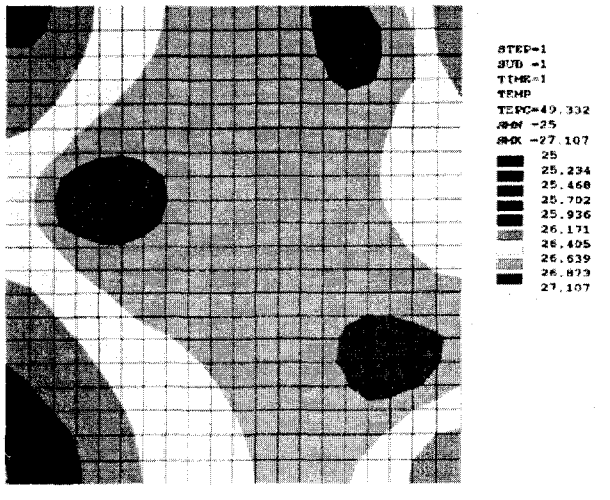

Figure 10. ANSYS finite-element thermal model generated for the microgyroscope package.

Fabrication and assembly of the microgyroscope package proceeded with particular attention paid to sealing and leak check operations. After the feed-throughs and pinch-off tube were installed into the enclosure, the assembly was checked for leak rate using standard helium leak check techniques. The enclosure leak rate was better than or equal to the resolution of the leak test (10^{-9} cc/sec or better). After the substrates were assembled and installed and the enclosure lid bonded and soldered in place, the assembly was placed in a vacuum chamber and outgassed for 24 hours @85° C in vacuum. After this time period, the vacuum in the chamber had stabilized at 10^{-7}torr. The pinch-off tube was then sealed, and the unit removed from the chamber.

CHARACTERIZATION

This paper presents the first data we have collected for a vacuum packaged microgyroscope with self-contained electronics. No external or "rack" electronics were utilized for these measurements which were done at ambient pressure and temperature. A first generation microgyroscope with a frequency split between drive and sense resonances of 7 Hz was used for this device. A turn-on time of 5 seconds was measured. Since the turn

on time depends on the Q of the drive resonance, the turn on time is likely to vary for future devices.

Packaged microgyroscope rotation data

The response of the microgyroscope to rotation rates between -2 deg/sec and +2 deg/sec is shown in figure 11. For this test, a TrioTech S347B rotation table with a resolution of 0.01 deg/sec was used to rotate the gyroscope package and a computer was used to record the output of the gyroscope as a function of rotation rate. Three consecutive tests are done to check for hysterisis and scale factor stability. Figure 12 shows the residuals for linear fits of all three rotation tests.

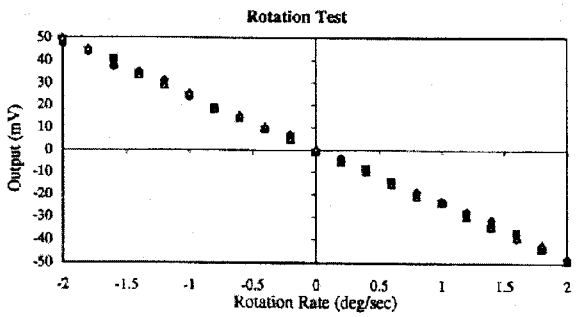

Figure 11. Rotation response of the packaged microgyroscope.

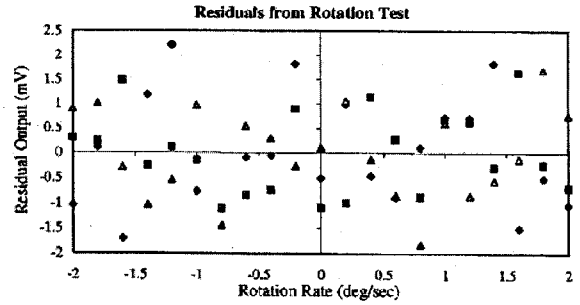

Figure 12. Residuals for linear fits of rotation tests of the packaged microgyroscope.

The Green chart, which plots the two-sampled standard deviation (square root of the Allan variance) as a function of the integration time, is shown in figure 13. The data from the packaged microgyroscope is compared with the previous results [1] obtained with external "rack" electronics. For the packaged microgyroscope, the rate white noise or angle random walk is 6.3 deg/$\sqrt{\text{hr}}$, the bias stability is less than 70 deg/hr, and the linear rate drift or rate ramp is 0.2 deg/hr/sec. The increased rate white noise of this packaged microgyroscope is due to the larger resonant frequency mismatch for this device. However, the rate ramp is reduced since the circuit tracks the small variations in the drive frequency.

Quadrature Error

The microgyroscope's performance as a rotation sensor greatly depends on how well the vibrating motion is controlled. Presently, a single loop is used to control the motion of the microgyroscope because it is assumed that the device is perfectly fabricated. Inevitably, there are device imperfections that result in an offset signal, or quadrature error, in the output of the gyroscope. We have repeatably shown that, for our bulk micro-machined gyroscope, the quadrature error does not result in amplifier saturation problems since it is small in magnitude compared to the Coriolis signals we are measuring. The quadrature error may be further minimized by the addition of a second control loop to ensure that the microgyroscope is vibrating correctly.

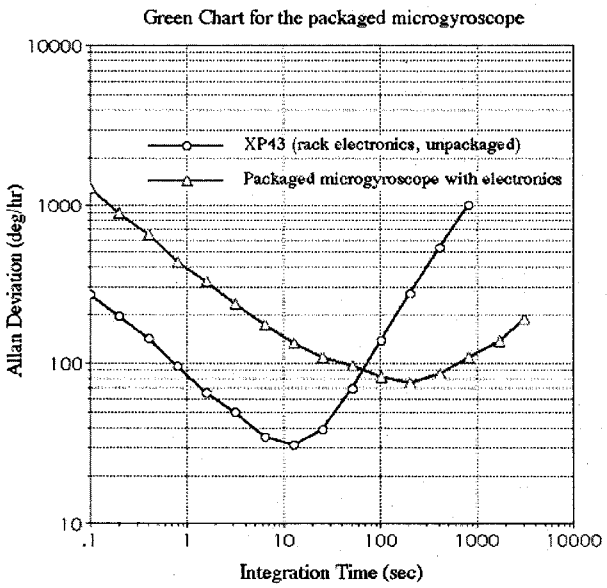

Figure 13. Green chart of the packaged microgyroscope.

Temperature Sensitivity

Our first generation of microgyroscopes [1] uses a quartz baseplate and a silicon vibrating structure. While this minimizes parasitic coupling, the difference in thermal expansion coefficient between the quartz and the silicon generates temperature dependent stresses in the resonating structure. These stresses change the resonant frequencies of the structure and, more importantly, the frequency difference between the drive and sense modes. We have measured a change in frequency of 1.4 Hz/degree for the drive mode, 3.7 Hz/degree for the sense mode and 5.0 Hz/degree for the up/down mode. This indicates that these microgyroscopes will not do well without temperature control.

The present generation of microgyroscopes uses a silicon baseplate and a silicon vibrating structure. In this design, only the electrodes and the bonding material generate temperature dependent stresses in the vibrating structure. We measured a change in frequency of 0.23 Hz/degree for both the drive and sense modes and 0.30 Hz/degree for the up/down mode. The results of this temperature testing are shown in figure 14 (the left peak is the two rocking modes while the right peak is the up/down mode). Notice that the drive and sense modes are overlapping in frequency at 1.4425kHz and that they do not separate with temperature changes.

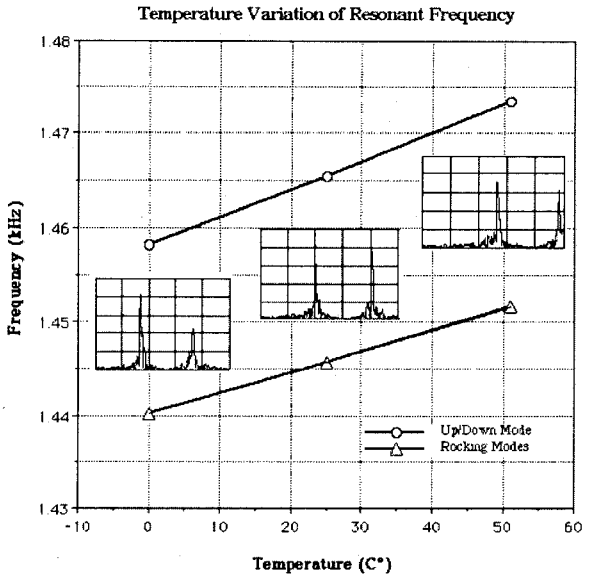

Figure 14. Temperature dependence of resonant frequency of the silicon clover-leaf structure.

FUTURE WORKS

Presently, we are continuing to improve the performance of the microgyroscope by refining the structure and fabrication process of the silicon mechanical resonator. A new clover-leaf microgyroscope with an integrated silicon post is under development that will simplify the assembly process and improve yield and performance. We are also working on force-rebalance feedback electronics that are necessary for the control of the degenerate-mode microgyroscopes. A new and much smaller Kovar package with glass-to-metal seals is being fabricated for the microgyroscope. This new package is designed to maintain pressure of less than 1 mtorr for over 3 years. Finally, a series of space qualification tests are being performed on the clover-leaf microgyroscope to determine the space worthiness of the device. These qualification tests include thermal cycling, radiation, vibration and shock. These tests are separated into two catalogues: survivability test and in-run test. Survivability test determines the maximum tolerance level of the device, while the in-run test determines the behavior of the device when subjected to the various environmental conditions. All these efforts will result in a robust and low cost microgyroscope system with improved performance of <1 deg/hr for space applications.

CONCLUSION

In this paper, we present performance data on a packaged silicon MEMS microgyroscope designed for space applications. The package housing the microgyroscope and most of the control electronics is approximately 1 x 1 x 0.7 inches in dimensions. The rest of the control electronics which includes the drive and lock-in amplifier circuitry are mounted outside the gyro box on a 1 x 1 inch circuit board. This packaged micro-gyroscope has a 7 Hz split between its drive and sense mode and a scale factor of 24mV/deg/sec, bias stability of less than 70 deg/hr, angle random walk of 6.3deg/√hr, and a rate ramp of 0.2deg/hr/sec. Recently we have demonstrated silicon clover-leaf structures with matched drive and sense resonant. These new structures have low temperature dependent frequency shift of 0.23 Hz/degree for both the drive and sense modes. With further improvement in the fabrication process, new packaging, and improved electronics the performance of this microgyroscope will be significantly improved.

ACKNOWLEDGMENTS

The authors thank Dr. Paul Maker and Richard Müller for the fabrication of e-beam photolithographic masks. Special thanks to Charles Cruzan and Sandy Chavez for the assembly of the microgyroscope package. The work described in this paper was performed by the Center for Space Microelectronics Technology, Jet Propulsion Laboratory, California Institute of Technology, and was sponsored by National Aeronautics and Space Administration, Office of Space Access and Technology.

REFERENCES

[1] T.K.Tang, R.C.Gutierrez, J. Wilcox, C. Stell, V. Vorperian, R. Calvet, W. Li, I. Charkaborty, R. Bartman, W. Kaiser, " Silicon Bulk Micromachined Vibratory Gyroscope", Tech Digest, Solid-State Sensor and Actuator Workshop, Hilton Head, S.C. pp.288-293, June 1996.

[2] M. Weinberg, J. Bernstein, J. Borenstein, J. Campbell, J. Cousens, B. Cunningham, R. Fields, P. Greiff, B. Hugh, L. Niles, J. Sohn, "Micromachining inertial instruments", SPIE Vol. 2879, pp.26-36, September 1996.

[3] P. B. Ljung, T. N. Juneau, and A. P. Pisano, "Micromachined Two Input Axis Angular Rate Sensor", *Proceedings of the ASME Dynamic Systems and Control Division,* DSC-Vol. 57-2, IMECE/ASME, pp.957-962, 1995.

[4] M.Putty, K. Najafi, "A Micromachined Vibratory Ring Gyroscope", Tech Digest, Solid-State Sensor and Actuator Workshop, Hilton Head, S.C., pp.213-220, June 1994.